PAPER • **OPEN ACCESS**

Carbon dots induced homeotropic alignment in a negative dielectric nematic liquid crystal material

To cite this article: Priscilla P *et al* 2024 *Nano Ex.* **5** 045008

NANO EXPRESS

PAPER

Carbon dots induced homeotropic alignment in a negative dielectric nematic liquid crystal material

Priscilla P[1], **Arvind K Gathania**[2], **Sandeep Kumar**[3,4], **Michael R Fisch**[5], **Jai Prakash**[6], **Supreet**[7], **Sanjeev Kumar**[8] **and Gautam Singh**[1]

[1] Department of Applied Physics, Amity Institute of Applied Sciences, Amity University Uttar Pradesh, Noida, 201313, India
[2] Department of Physics and Photonic Science, National Institute of Technology, Hamirpur, Himachal Pradesh, 177005, India
[3] Raman Research Institute, C.V. Raman Avenue, Sadashivanagar, Bengaluru, 560080, India
[4] Department of Chemistry, Nitte Meenakshi Institute of Technology, Yelahanka, Bengaluru, 560064, India
[5] College of Aeronautics and Engineering, Kent State University, Kent, OH, 44242, United States of America
[6] Department of Physics, Aligarh Muslim University, Aligarh, 202002, India
[7] Department of Physics, Amity School of Applied Sciences, Amity University Haryana, 122413, India
[8] Department of Physics, Chandigarh University-Gharuan, Mohali, 140413, India

E-mail: mfisch@kent.edu **and** gsingh6@amity.edu

OPEN ACCESS

RECEIVED
28 May 2024

REVISED
26 September 2024

ACCEPTED FOR PUBLICATION
29 October 2024

PUBLISHED
13 November 2024

Keywords: nematic liquid crystal, negative dielectric anisotropy, homeotropic alignment, carbon dots, liquid crystal composites

Supplementary material for this article is available online

Abstract

Recently, doping guest materials such as quantum dots (QDs) into liquid crystals (LCs) has been of great interest since their addition substantially enhances the properties of LC and opens new avenues for scientific advancement. Here, we report the induction of homeotropic alignment in cells without alignment layers of the negative dielectric nematic liquid crystal, N-(4-Methoxybenzylidene)-4-butylaniline (MBBA) by doping with carbon dots (CDs ~2.8 ± 0.72 nm). The CDs-MBBA composites (CDs concentration: 0.002, 0.01, 0.03, 0.1 and 0.3 wt%) were investigated using optical polarising microscopy, electro-optical and dielectric techniques. Polarizing optical micrographs and voltage dependent optical transmission revealed the induced homeotropic alignment for all the composites under investigation. Interestingly, the least concentrated sample, 0.002 wt% exhibited partial homeotropic alignment. However, due to light leakage, the optical transmission value below threshold voltage was relatively higher than the rest of the composites. MBBA is a negative dielectric material, hence the application of a voltage across the cell was able to switch the alignment from a dark to a bright state for all composites. However, above a certain voltage (>threshold voltage), the bright state produced some instabilities. The value of dielectric permittivity was observed to decrease with increasing concentration, confirming the effect of CDs in producing homeotropic alignment in MBBA. Measurements as a function of temperature were conducted to examine the thermal stability of the induced alignment. The alignment was found to be stable throughout the nematic phase of MBBA. The induction of such alignment without conventional alignment (i.e., rubbing of polyimides) technique can be helpful in addressing the evolving display demands by making liquid crystal displays (LCDs) and other display devices cost effective.

1. Introduction

In the world of display technologies, alignment of nematic liquid crystal (NLC) remains one of the most crucial factors determining the optical effectiveness of the device. The NLC of calamitic molecules is the simplest LC phase characterized by the long axis of the molecules orienting themselves on average in a specific direction represented by a unit vector $\mathbf{n} = -\mathbf{n}$ [1, 2]. Alignment of NLC at a planar substrate can be majorly classified as one of two types: homogeneous (planar) and homeotropic (vertical). Homogeneous alignment is when the director (**n**) is oriented parallel to the substrate's surface. When **n** is oriented perpendicular to substrate the LC is

referred to as homeotropically aligned [3]. NLCs exhibit two types of dielectric anisotropy ($\Delta\varepsilon = \varepsilon_{\parallel} - \varepsilon_{\perp}$) i.e., positive ($\Delta\varepsilon > 0$) and negative ($\Delta\varepsilon < 0$), wherein $\varepsilon_{\perp}$ and $\varepsilon_{\parallel}$ denote the perpendicular and parallel components of the real dielectric permittivity, respectively [4, 5]. For the fabrication of vertical switching devices, a positive anisotropic NLC is filled into a sample cell with two substrates that promote homogeneous alignment, while a negative anisotropic NLC is employed in a sample cell with homeotropic alignment. A negative dielectric anisotropy NLC has an extra advantage over its positive counterpart since its aligned at right angles to the substrates hence it does not show a change in the inclination angle as the substrate is rotated in the plane [6]. They also exhibit wider viewing angle, improved reliability, shorter response time, higher optical contrast, and fewer flicker issues [7] than positive anisotropy devices. This is why negative dielectric anisotropic NLC materials are preferred for the fabrication of display devices by industries [8].

Studies have shown that there are several techniques for obtaining alignment of NLCs at substrates. The most commonly used method to obtain homogenous alignment is the traditional rubbing process in which the substrates (often glass) are initially coated with a polyimide layer and later on rubbed using a synthetic cloth to produce microgrooves that help in orienting the molecules towards a certain direction. However, this conventional technique has some serious flaws such as generation of debris, local defects in displays due to uneven degradation of rubbing rollers, formation of static charges, etc. Similarly, in order to achieve a homeotropic alignment surface active agents like alkyl silanes, lecithin, etc are used [9, 10]. These methods have been widely used by the display industries in the manufacturing of LC devices because of their cost effectiveness and remain as a fast and simple method to obtain reliable alignment. Due to such reasons attaining a uniform and reliable alignment of NLC materials remains a common theme of research in the LC community. Researchers have proposed some other techniques of alignment for instance: atomic/ion-beam irradiation [11–14], Photoalignment [15], UV-light irradiation [9], Oblique evaporation method [16], Electric/Magnetic field [17], Langmuir–Blodgett (LB) film method [18], and dispersion of nanoparticles (NPs, particles with size range between 1–100 nm in at least one of its dimensions) [19–24].

Achieving uniform alignment took a new resurgence since the development of NPs [19, 20, 25]. The change in properties upon adding NPs to LC motivated scientists to mix NPs in NLCs and monitor their effect on NLC properties. The result of this incorporation was promising and provided a ray of hope in eliminating the conventional rubbing techniques. In an attempt to induce alignment, scientists have conducted various studies on the subject of NPs dispersion in a negative dielectric NLC in an unaligned ITO sample cell. For instance, Jeng *et al* [26] reported that the doping of POSS (polyhedral oligomeric silsesquioxane) NPs (0.7– 30 Å) induced homeotropic alignment in negative dielectric NLC (MLC6882, $\Delta\varepsilon = -3.1$) at a concentration >3 wt%. Further investigation also showed that such induced homeotropic alignment is attributed to the adhering of the POSS NPs to the inner surface of the LC substrates as they diffuse into the cells [27]. Similarly, Chinky *et al* [28] has reported the achievement of a good quality homeotropic alignment in NLC (MJ98468, $\Delta\varepsilon = -4$) by the doping of ZnO NPs (<50 nm) whereby they observed a lowered threshold voltage and enhanced contrast ratio (~12.4%) of the composites at a concentration of 0.3%wt ZnO in NLC. In an exceptional work, Lim *et al* [29] induced homeotropic alignment of a negative NLC ($\Delta\varepsilon = -4$) by growing ZnO nanorods (L: 502 ± 117.64 nm, Dia: 24.1 ± 4.25 nm) on the ITO coated substrates; for a concentration of 1.0 mM $Zn(NO_3)_2$ the composite was able to achieve a perfect and clear dark state. In a similar study, Dogra *et al* [30] did a comparison on the effect of coating and doping silica NPs (~80 nm) on the alignment of NLC (LC-BYVA-01, $\Delta\varepsilon = -4.89$). It was observed that both produced an equally good quality homeotropic alignment in an ITO sample cell with no alignment layers at a concentration of 0.3wt%.

Recently QDs have gained much attention due to their phenomenal optical and electronic properties. Having a size ranging from 2–10 nm these QDs have garnered much attention since they are able to emit lights of different colors under UV illumination [31, 32]. Toxicity is one of the major issues faced by the conventional semiconducting QDs (CdS, CdSe, CdTe, etc) [33] and hence, more focus has been given to eco-friendly QDs [34]. Since the results obtained using semiconducting QDs-NLCs composites were rather promising, scientists then tried to explore the possibilities of dispersing ecofriendly QDs into a negative dielectric NLC and observed the effect they produced in the alignment of the NLC when infiltrated into an unaligned ITO sample cell. In the first of such investigations, Lee *et al* [35] reported that dropcasting a $CuInS_2$-ZnS QDs (~2.2 nm) NLC ($\Delta\varepsilon = -4.2$) composite results in the formation of homeotropic alignment at 0.01 and 0.02 mol l^{-1} concentration of QDs. They attributed this to the formation of 1-D chain like QD clusters which act as microgrooves on the substrates aiding the alignment of NLC matrix. Thereafter, Son *et al* [36] demonstrated the tendency of octadecylamine-functionalized graphene QDs (O-GQDs ~1.48 nm) to self-assemble and form a nanostructured layer at the interfacial surfaces with the ITO coating results in the spontaneous homeotropic alignment of a negative NLC ($\Delta\varepsilon = -3.1$). Moreover, the significantly modulated response time was also reported by the authors for 0.05wt% GQDs-NLC composite.

CDs are one such eco-friendly QDs that are of increasing interest [37]. CDs are able to portray themselves as a potential competitor to the traditional QDs because of its budget friendly and simple routes of synthesis, low

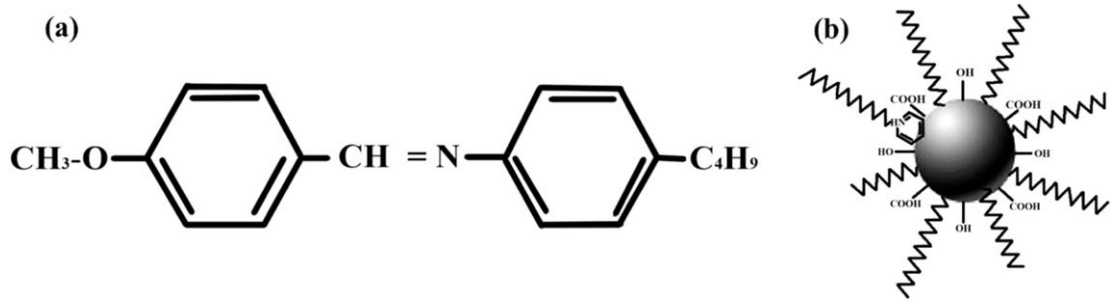

Figure 1. Molecular Structure of (a) MBBA, NLC and (b) Carbon dots (CDs) [44].

toxicity, surface passivation, eco-friendliness, surface functionalization, and an overall level of fluorescence comparable to their semiconducting counterparts [33]. Interestingly, CDs are being used to tune the physical properties of NLCs. For instance, the first work was reported by Urbanski *et al* [38] where they dispersed carbon QDs (CQDs, 2.5 ± 0.5 nm) in NLC (Felix-2900–03) material which was eventually infiltrated into a planar aligned ITO coated sample cell. Planar alignment was recorded for concentrations up to 2.5wt% and beyond which at 5wt% a combination of homeotropic and partial planar alignment was observed. The homeotropic alignment was stable only deep in the nematic phase (low temperature) and turned to planar alignment at higher temperatures just like the rest of the lesser concentrated composites (⩽2.5wt%). The authors attributed this observed homeotropic alignment to the increased pretilt angle (∼8°) produced as a result of CDs having settled at the planar anchored interfaces. Rastogi *et al* [39] doped oil palm leaf (OPL) based carbon NPs (5.67 nm) in NLC (E 48, $\Delta\varepsilon = +12.5$), and they utilized graphene oxide NPs (0.4 wt%) as an aligning layer in ITO sample cells to achieve homeotropic alignment of the composites. Addition of OPL NPs produced planar alignment, and the brightest state was obtained for the highest concentration of 0.3 wt/wt%. In their another work [40], they have reported the homogenous distribution of CQDs (4–6 nm) in the same host NLC (E 48, $\Delta\varepsilon = +12.5$) optically and in yet another study [41] using the same materials they tried injecting the CQDs-NLC composites in an unaligned sample cell and reported irregularities and low contrast in the alignment obtained, so they filled the composites in planar aligned sample cells and found improved molecular alignment, contrast and uniform dispersion of CQDs in the NLC under investigation. A change in the color of the composites was attributed to the variation in the birefringence with temperature. Most recently, we have reported the impact of organosoluble CDs (∼7–8 nm) on the alignment of planar anchored 5CB, NLC, and demonstrated that for concentration ⩾0.3wt% the CDs were able to induce a uniform and stable homeotropic alignment throughout the nematic phase [42]. Moreover, tunable ionic conductivity in these CDs-5CB composites was also recently reported by our group [43].

Summing up the above review gives a clear indication that currently there are no reports on the induction of stable homeotropic alignment in a negative dielectric NLC material using CDs. In this work we report induced homeotropic alignment in a negative dielectric NLC (MBBA) using CDs in an ITO sample cell without alignment layers. Interestingly, induced homeotropic alignment of NLC was observed even at the very low concentration of dopant CDs (i.e. 0.002 wt%). Moreover, the confirmation of induced homeotropic alignment and its stability throughout the nematic phase were studied by using polarizing optical microscope, electro-optical techniques, and dielectric spectroscopy.

2. Experimental details

2.1. Materials used and preparation of CDs-NLC composites

In this work, we employed the negative dielectric NLC material, MBBA (N-(4-Methoxybenzylidene)-4-butylaniline) purchased from Tokyo Chemical Industry (India) Pvt. Ltd, division of Tokyo Chemical Industry. It was used as received and the molecular structure is shown in figure 1(a). Organosoluble functionalized CDs produced by the one pot selective synthesis mechanism [44] were used as dopants which was fully characterized by Mahesh *et al* [45], its formation and structure was studied by Minervini *et al* [46] as shown in figure 1(b). Additionally, we have also characterized the size of CDs employed using HRTEM which is discussed in results section. The phase sequence of MBBA is reported as: **I** (41 °C) **N** (22 °C) **Cr**, here **I**, **N** and **Cr** symbolizes isotropic, nematic and crystal phases, respectively [47]. For the preparation of composites, we initially blended CDs in chloroform to prepare a 0.1 w v^{-1}% solution that was subsequently added into 5 mg of MBBA at various proportions in order to make five distinct concentrations 0.002, 0.01, 0.03, 0.1 and 0.3 wt% of CDs. These prepared composites were ultrasonicated for two hours to obtain a homogenized mixture whereafter they were

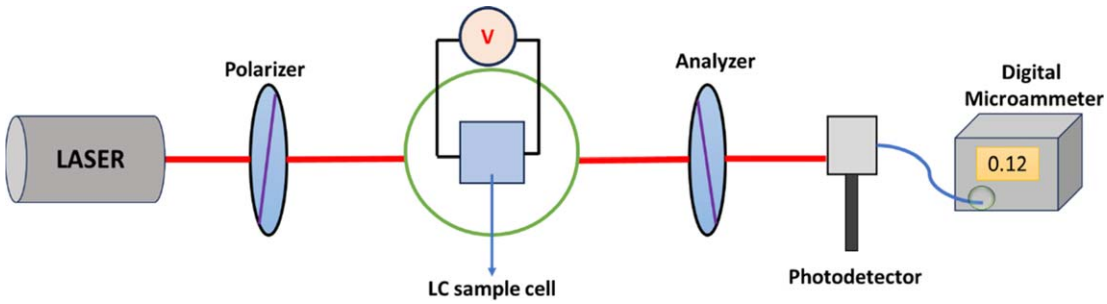

Figure 2. Schematic diagram of the electro-optical set up used for voltage-dependent optical transmission measurement.

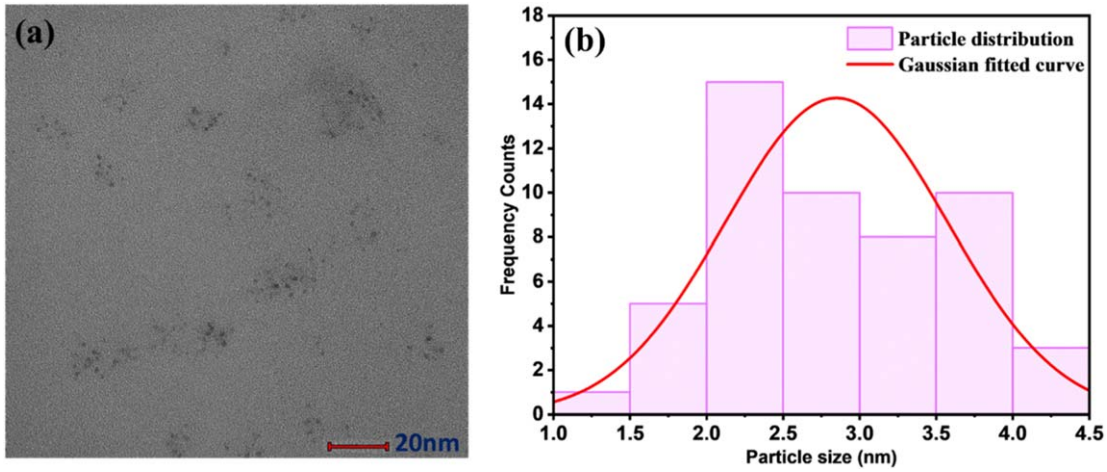

Figure 3. (a) HRTEM image and (b) Particle size distribution of CDs. The scale bar is 20 nm.

heated for one hour in the oven at 70 °C to evaporate the chloroform from the composites. These composites were finally infiltrated into unaligned ITO sample cells (i.e., without rubbed polyimide) of thickness 4 μm purchased from Instec Inc., USA for the optical, dielectric and electro-optical investigations.

2.2. Characterization techniques

To investigate the alignment of CDs-MBBA composites and pure MBBA, a cross-polarized optical microscope (CENSICO International 13809, India) in conjunction with an image camera (AmScope, FMA050) was employed. An LCR meter (nF, ZM2376, Japan) with a frequency range of 100 Hz–5.5 MHz and an oscillator voltage of 300 mV was used to conduct the dielectric measurements with and without an external LC orienting voltage. A customized hot stage linked to a circulating water bath (Thermotech, AQS-WB-200, India) that provides an accuracy of ±0.5 °C was used for regulating the temperature of the unaligned ITO sample cells. Electro-optical measurement i.e., voltage-dependent optical transmission [5, 27, 28] was done using diode laser power supply (Optochem International, 3V, 635 nm, India) passed through the LC cells placed between two cross polarisers linked with a dual output DC regulated power supply (50V/5A). Further, the transmitted light is fed to the photodetector (Indosaw, SK045, India) and then directed to a digital microammeter (Nisco India Limited, DMA-02, India) for measurement of voltage-dependent optical transmission intensity (figure 2). The size distribution of CDs has been obtained using high resolution transmission electron microscope (HRTEM, Tecnai G20, USA) applied with an accelerating voltage of 200 kV.

3. Results and discussions

3.1. HRTEM analysis of carbon dots

Figure 3(a) demonstrates the acquired image of CDs using HRTEM where the particles are observed to have a quasi-spherical morphology. The average size of CDs has been analyzed using ImageJ software where more than 50 particles are considered for the estimation. Thereafter, the acquired data was processed in Origin software

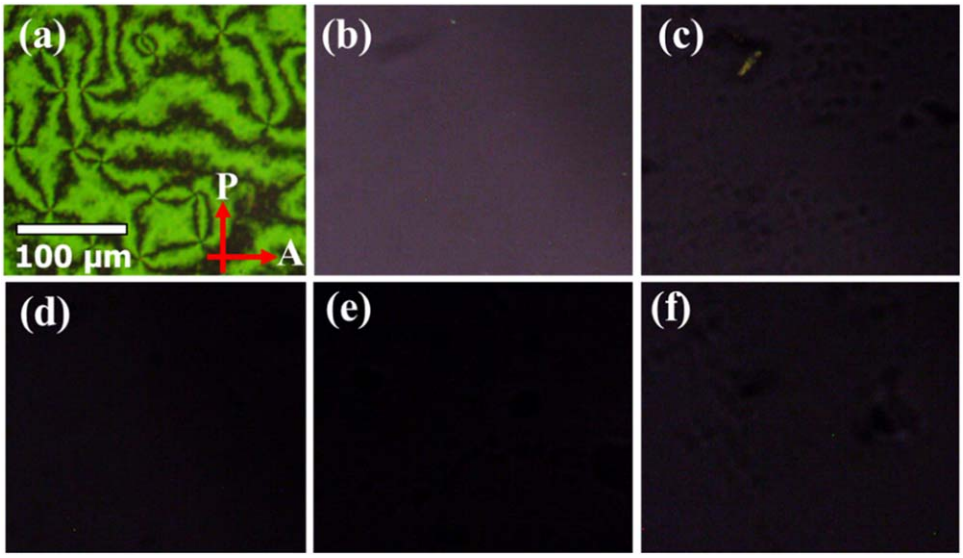

Figure 4. Cross-polarised optical textures for (a) 0.00 wt%, (b) 0.002 wt%, (c) 0.01wt%, (d) 0.03 wt%, (e) 0.1wt% and (f) 0.3 wt% of CDs-MBBA composites at T = 32 °C. P and A indicate the polarizer and analyzer, respectively. The scale bar is 100 μm.

and an average distribution was obtained (figure 3(b)). The histogram made for particle size distribution is best fitted with Gaussian function and the size of CDs is confirmed to be 2.8 nm with a standard deviation of ±0.72.

3.2. Optical texture and electro-optical studies

Figure 4 exhibits the optical textures of Pure MBBA and CDs-MBBA composites in an unaligned ITO sample cell at T = 32 °C. figure 4(a) displays a Schlieren texture generally observed in the samples exhibiting the N phase which confirms that filling of MBBA in the cell did not induce any type of alignment to the NLC molecules. Surprisingly, the addition of CDs in NLC generates a partial homeotropic alignment even at the lowest concentration of 0.002 wt% (figure 4(b)). As the concentration of CDs is increased to 0.01 wt%, the darkness of texture slightly improved albeit some defects are seen (figure 4(c)). Interestingly, 0.03 and 0.1 wt% composites showed absolute dark texture (figures 4(d) & (e)) demonstrating excellent homeotropic alignment induced by CDs in MBBA, NLC. However, increasing the concentration to 0.3 wt% shows the presence of some defects in the optical texture (figure 4(f)) that could be attributed to the plausible aggregation of CDs due to their higher concentration. Absence of any alignment layer on the substrates surface facilitates the CDs interaction with ITO inducing homeotropic alignment. We anticipate that the plausible interaction of CDs with ITO substrates plays a major role in controlling the arrangement of molecules. It is worth pointing out here that 0.002wt% concentration of CDs turns out to be the lowest concentration reported till now which could induce homeotropic alignment in a negative dielectric NLC material.

The interaction between MBBA LC molecules and CDs have been demonstrated through a schematic model in figure 5 where initially the MBBA molecules are in unaligned state as observed in the optical texture in figure 4(a). Since the alkyl groups in CD make them more hydrophobic than bare ITO layer, we believe that the hydrophilic components like carboxyl and hydroxyl groups organizes themselves on the ITO layer and the hydrophobic alkyl group arranges themselves towards the LC molecules [36]. The alkyl groups that comes in contact with LC molecules produce not only their reorientation to homeotropic state but also gives them proper stability to maintain this alignment amidst varying thermal effects. The self-assembly nature of LC molecules helps in penetrating this state of alignment in the bulk of the sample. For lower concentrations (<0.03 wt%), the coverage of CDs on the ITO layer is very less due to which the LC molecules fail to show a complete reorientation thereby inducing light leakages in the sample. However, for increased concentrations (⩾0.03 wt%) as depicted in schematic, the sedimentation of larger number of CDs covers a greater ITO area. This wide coverage leads to the formation of a hydrophobic surface similar to those generated by conventional PI layers that control the orientation of LC molecules [36]. Hence, the similarity of CDs in acting as conventional PI layers produces a well-defined uniform homeotropic alignment at high concentrations thereby eliminating the costly alignment layers. Moreover, the dipolar interaction among CDs and MBBA molecules could be another probable reason for the observed induced homeotropic alignment.

Furthermore, in a negative dielectric material applying voltage enables the molecules to switch from homeotropic to planar state. Figure 6 demonstrates the effect of varying voltage on the textures of CDs-MBBA composites.

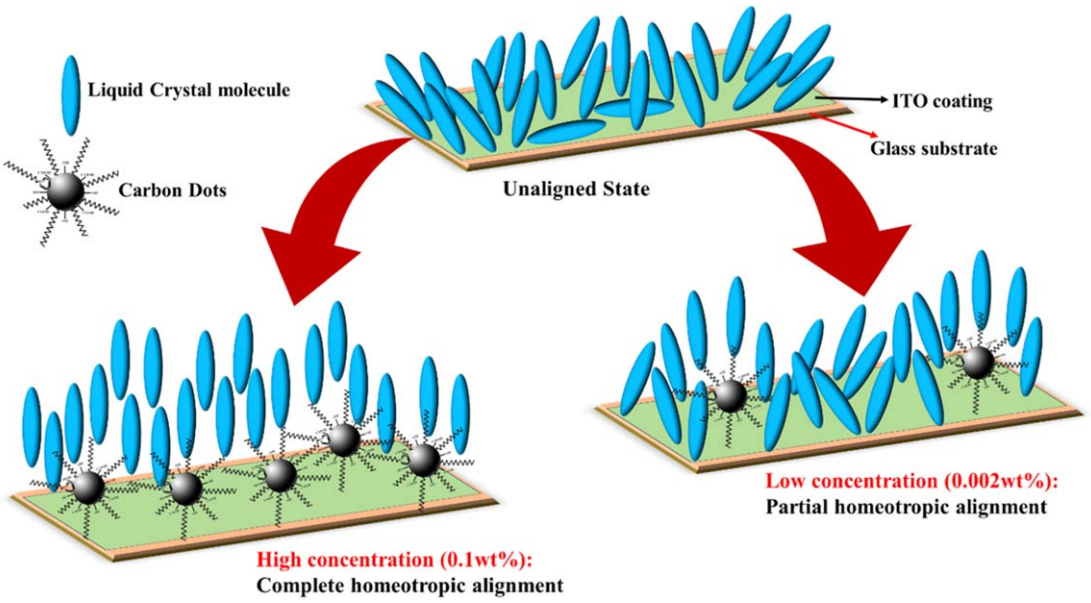

Figure 5. Schematic model representing the induced homeotropic alignment produced by the interaction of MBBA LC molecules with Carbon dots in an ITO coated glass substrate with no alignment layer.

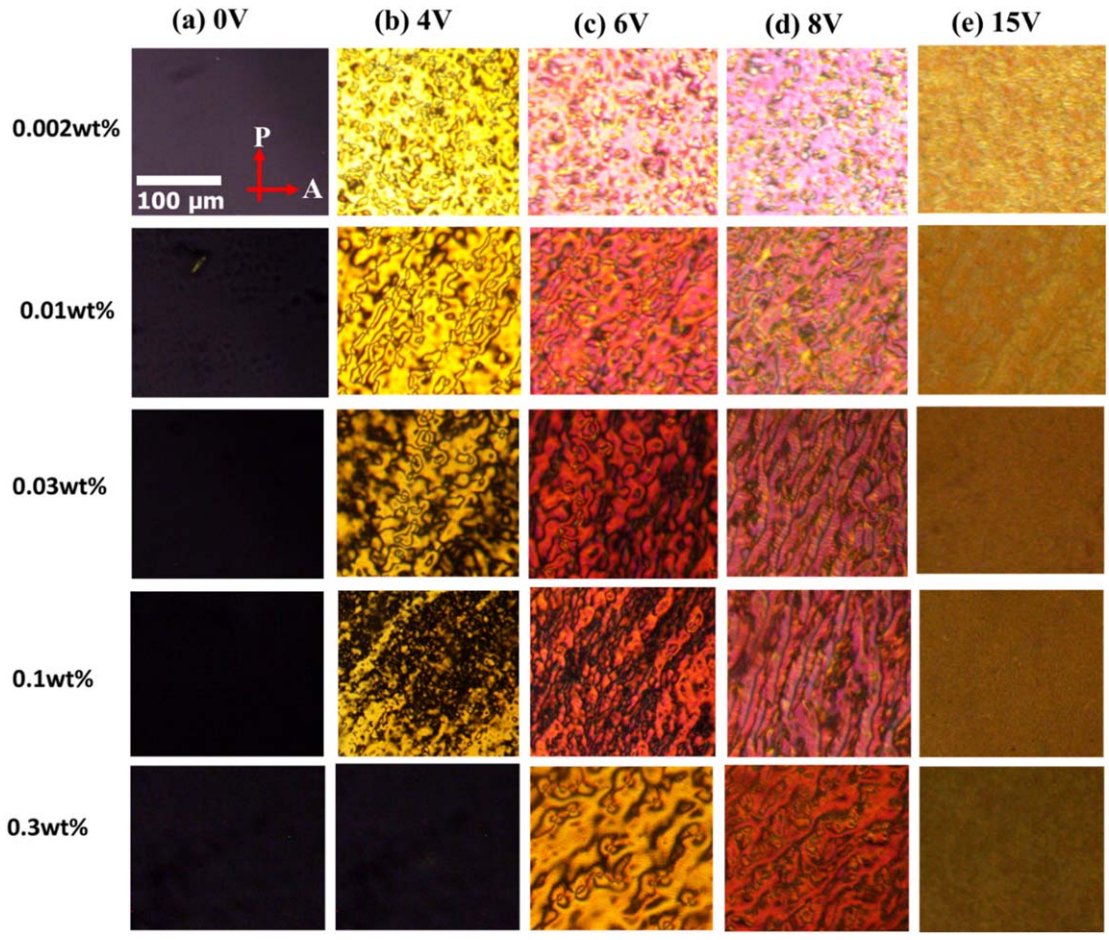

Figure 6. Optical textures for varying voltages (a) 0 V, (b) 4 V, (c) 6 V, (d) 8 V and (e) 15 V of CDs-MBBA composites at a constant temperature of T = 32 °C. P and A indicate the polarizer and analyzer, respectively. The scale bar is 100 μm.

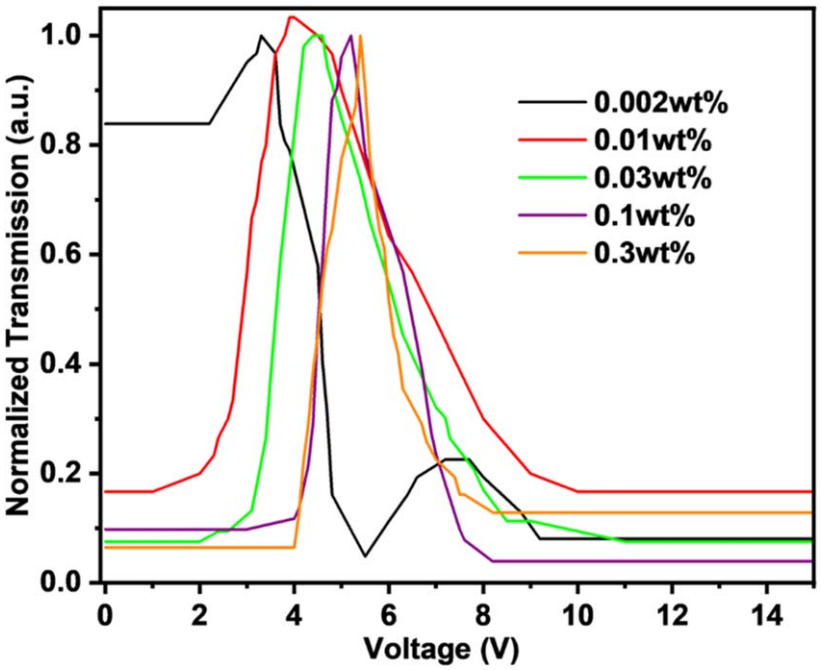

Figure 7. Voltage dependent optical transmission of CDs-MBBA composites at T = 32 °C.

As observed in figure 6, application of a voltage could switch the molecules to a bright state however, for all the CDs-MBBA composites these bright states did not have any uniformity. They also produced instabilities in the texture at high voltages [27, 28]. The analysis of such behavior led to the conclusion on the non-availability of any pre-existing alignment layers in the sample cells allowing the molecules to orient in random directions when an external voltage is applied and this eventually disrupts the bright state with instabilities. ITO substrates with some pretilt angle are beneficial because when the molecules are switching to the bright state the pretilt will align the molecules to form a planar alignment rather than arranging themselves randomly. Four and two brush defects can be seen in the texture when applied with voltage indicating the nematic phase of the LC molecule. It can also be observed that for the highest concentration 0.3wt%, the switch can be seen happening for voltages above 4V implying an increase in the threshold voltage. For comparison, the voltage dependent optical textures of Pure MBBA and 0.1 wt% CDs-MBBA composite filled homeotropically anchored ITO sample cells are demonstrated in figure S1. It appears that the quality of homeotropic alignment in unaligned ITO sample cell filled with 0.1 wt% composite is better than Pure MBBA and 0.1 wt% composite filled in homeotropic aligned ITO sample cells. However, the switched planar state does not have proper planar alignment (figure S1) as in case of unaligned ITO sample cells with CDs-MBBA composites (figure 6).

Figure 7 shows the variation in the intensity of transmitted light with changing voltage, and the alignment allows a change from a dark to a bright transmitted light state. However, stability of the bright state doesn't remain uniform, and the intensity falls back to the ground state at higher voltages [27]. Due to light leakage, the intensity of 0.002 wt% composite is higher than the remaining composites as previously demonstrated through optical texture (figure 4(b)). An increased threshold voltage (V_{th}) is associated with increasing concentration of CDs. A V_{th} of 4.1 V is observed for 0.3wt% composite, whereas it is lower for the remaining composites; this is analogous to the voltage dependent optical texture shown in figure 6. The observed increase in V_{th} could be attributed to the enhancement in homeotropic anchoring of host MBBA molecules by the increasing concentration of dopant CDs (figure 5). A temperature dependent study was conducted to check the stability of the homeotropic alignment induced by CDs in CDs-MBBA composites and it was seen that the alignment is highly stable throughout the N phase range as shown in figure S2.

3.3. Dielectric spectroscopic study

Dielectric studies are usually conducted to investigate and understand the dynamics of molecules in NLC materials and their composites with nanomaterials [48–54]. Here, the dielectric measurements were done on the unaligned ITO sample cells filled with CDs-MBBA composites with homeotropic alignment induced by CDs.

Figure 8 represents the frequency dependent variation of dielectric permittivity of CDs-MBBA composites at a constant temperature of 32 °C. At low frequency region ($\leqslant 10^3$ Hz) a slight increase in ε' can be observed that is attributed to the low frequency relaxation of the composites and ionic effects. Thereafter, the value of ε' remains

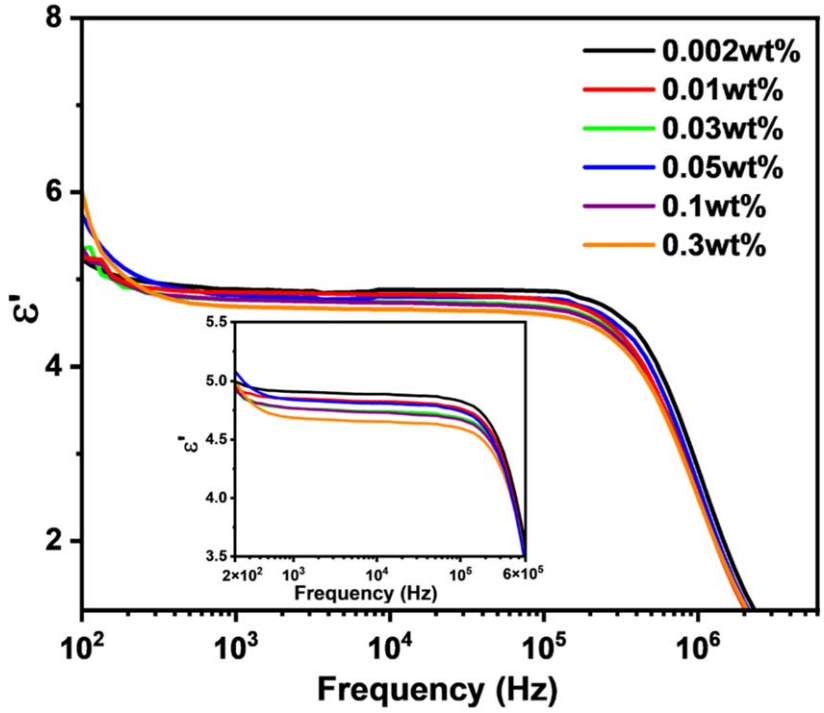

Figure 8. Frequency dependent real dielectric permittivity (ε') of CDs-MBBA composites at T = 32 °C (Inset shows the enlarged image).

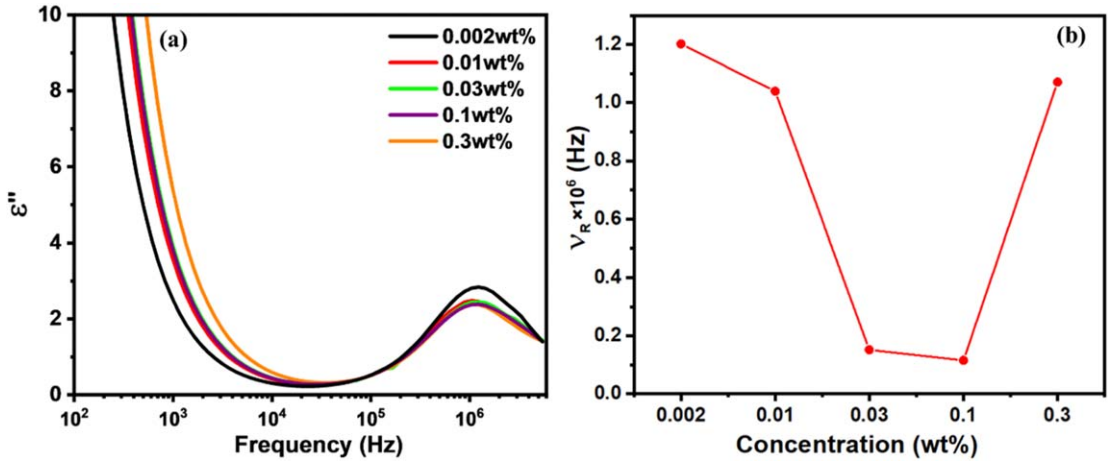

Figure 9. (a) Frequency dependent dielectric loss (ε'') for CDs-MBBA composites, and (b) Concentration dependent short axis relaxation frequency at T = 32 °C.

constant with changing frequency until 10^5 Hz and decreases for frequency above 10^5 Hz. The inset of figure 8 shows that with increasing concentration of CDs the value of ε' decreases, whereby for 0.002 wt% the observed value is 4.88 while for 0.3 wt% a value of 4.65 is observed. This can be attributed to the quality of homeotropic alignment produced by CDs with increasing concentration. Since the host LC used here is a negative dielectric material the value of the parallel component of the real dielectric permittivity ($\varepsilon_{\parallel}$) has to be lower than the perpendicular component ($\varepsilon_{\perp}$).

To confirm the induced homeotropic alignment, dielectric loss (ε'') was examined and as can be noticed in figure 9(a) that all composites manifested the short axis relaxation peak [5]. A shift in the relaxation peak towards lower frequency side can be seen with increasing CDs concentration. From figure 9(b) we can observe that the relaxation peak for 0.002 wt% is at 1.2×10^6 Hz which decreases to 0.1×10^6 Hz for 0.03 wt% and 0.1 wt% due to increased homeotropic alignment induced by CDs. However, for 0.3 wt%, the relaxation peak frequency

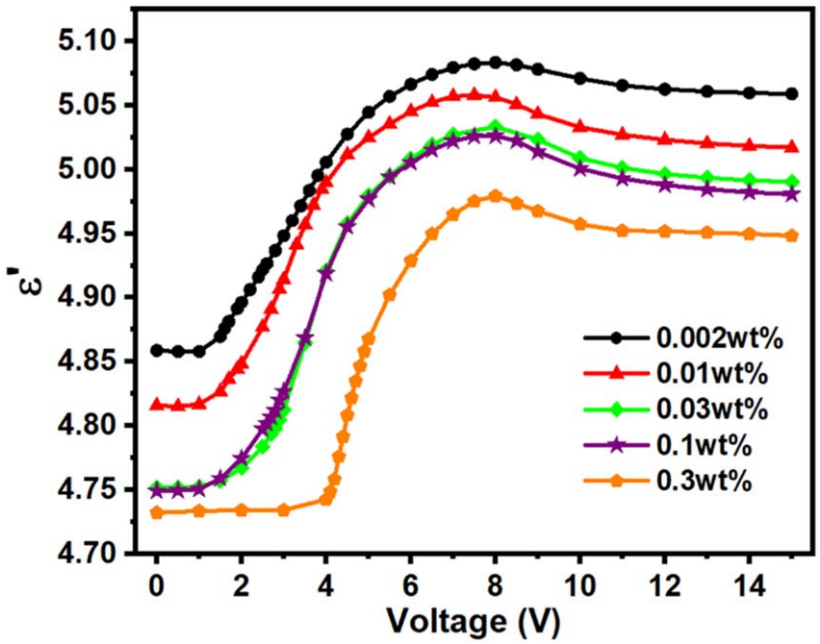

Figure 10. Voltage dependent real dielectric permittivity (ε') of CDs-MBBA composites for a constant frequency of 10 kHz at T = 32 °C.

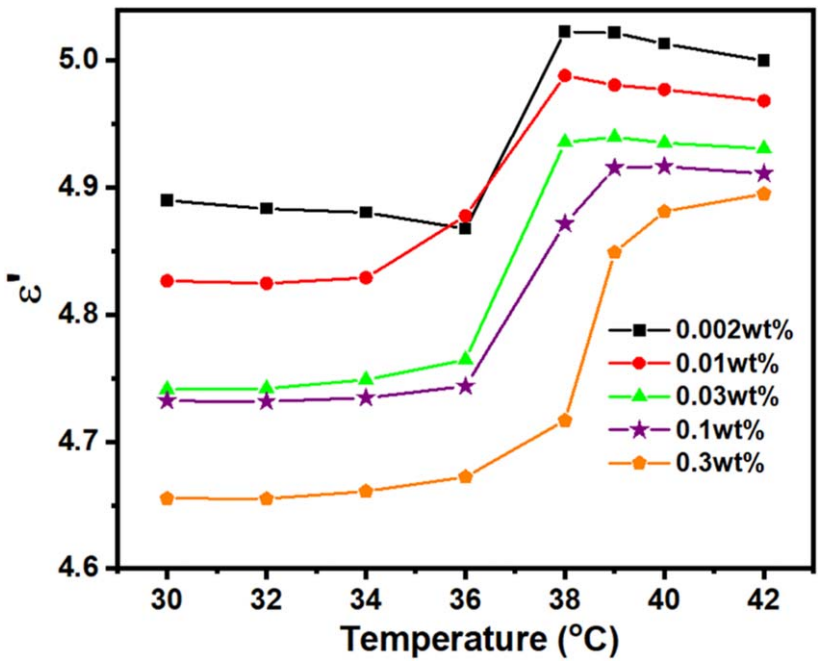

Figure 11. Temperature dependent real dielectric permittivity (ε') of CDs-MBBA composites at a constant frequency of 10 kHz.

shifts back to the value exhibited by 0.002wt%. Analysis of the dielectric loss gives a valid credibility on the induced homeotropic alignment by CDs in host MBBA, NLC.

An orientating voltage was applied to understand the variation of permittivity as the molecules switched orientation from the homeotropic to the planar state (figure 10). As seen from the graph, the switched planar state was not stable. The value of permittivity increases with voltage initially and then reaches a saturation state; however, the graph shows that the state of saturation is not constant but exhibits a drop in value that we accredit to the instabilities creeping in the texture at higher voltages. When the applied voltage is greater than 8V, the permittivity of the composite decreases, which is due to the non-availability of a pre-existing anchoring on the substrates and also due to the inherent property of CDs to show an enhanced conductivity [55]. Enhancement in

the conductivity by the doping of CDs can play a significant role in the instability produced in textures at high voltages; the textures reveal that application of high external voltage is not favorable for the CDs used in this system. A relatively lesser threshold voltage was observed for all composites except for 0.3wt% which corroborates well with the optical texture shown in figure 6.

After conducting dielectric studies at a single temperature, we explored the effect of varying temperature on the value of ε' of CDs-MBBA composites. As can be observed in figure 11, the value of permittivity remained relatively independent (+/−4%) of wt% CDs with changing temperature in the N phase. This is attributed to the thermal stability in the homeotropic alignment produced by CDs. This stability has been shown optically also in figure S2. Moreover, the clearing temperature ($T_{N\text{-}I}$) for pure unaligned MBBA sample was found to be 40 °C which got reduced by ~2 °C in case of lower concentrations (⩽0.03 wt%) however for higher concentrations the $T_{N\text{-}I}$ exhibited an increase (figure 11). For 0.3 wt% concentration, the $T_{N\text{-}I}$ became 40 °C akin to that of pure sample (table1, Supplementary). Such induced homeotropic alignment of a negative dielectric NLC that are thermally stable even at such low concentration of CDs can be used in the fabrication of thermal sensors and adaptive lenses.

4. Conclusion

In the present work, we have demonstrated induced homeotropic alignment of a negative dielectric NLC (MBBA) when doped with organosoluble CDs that has been filled in a sample cell with ITO electrodes but without alignment layers. Such induced homeotropic alignment has been confirmed through polarizing optical microscope, dielectric spectroscopy, and electro-optical techniques. Optical textures confirmed the induced homeotropic alignment even at the lowest concentration of 0.002 wt% and an increase in concentration of CDs to 0.1wt% produced a better homeotropic state in the composites. Application of external voltage was able to switch these homeotropically aligned composites to their bright states with some instabilities. Switching was observed electro-optically and it was seen that the composite with the highest CDs concentration (0.3 wt%) produced an increased V_{th} that is attributed to the stronger homeotropic alignment induced by CDs. Through dielectric measurements, we also observed that the value of dielectric permittivity decreased by ~5% with increasing concentration since MBBA being a negative dielectric NLC material. The 0.3wt% composite showed the least value of permittivity out of all the composites under all studied conditions. Attainment of such induced homeotropic alignment at low concentrations of CDs (<0.3 wt%) certainly manifests the effective interaction of CDs with LC material specially in the absence of any alignment layers. The short axis relaxation of the molecule was also probed, and it was observed that all composites demonstrated homeotropic alignment due to the observance of short axis peak and a shift in the relaxation peak was observed with increasing concentration of CD less than 0.1%. Such induced homeotropic alignment remained thermally stable which was confirmed both dielectrically and optically. Such thermally stable induced homeotropic alignment can be useful in LCDs, optical shutters, smart windows, and photonic devices.

Acknowledgments

Authors are thankful to Prof. Sunita Rattan, Director, Amity Institute of Applied Sciences (AIAS), Amity University Uttar Pradesh (AUUP), Noida for her continuous encouragement and interest in the present work. We are also grateful to AUUP, Noida for providing the research facilities to carry out the present research work. Priscilla P would like to thank UGC for the fellowship awarded under the scheme Savitribai Jyotirao Phule Single Girl Child Fellowship (SJSGC 2022-2023). Jai Prakash and Gautam Singh are grateful to the Council of Science and Technology (CST), U. P., India for financial assistance under CST, U. P. funded research project (Project ID: 1960). Supreet, Sanjeev Kumar and Gautam Singh acknowledge the support provided under SERB SURE Grant no. SUR/2022/004020 of Govt. of India.

Data availability statement

Not applicable. The data that support the findings of this study are available upon reasonable request from the authors.

ORCID iDs

Michael R Fisch https://orcid.org/0000-0002-0462-4967
Jai Prakash https://orcid.org/0000-0002-1100-0749

Sanjeev Kumar https://orcid.org/0000-0002-7560-1973
Gautam Singh https://orcid.org/0000-0002-7514-1196

References

[1] de Gennes P G, Prost J and Pelcovits R 1995 The physics of liquid crystals *Phys. Today*. **48** 70–71
[2] Singh G, Kumar S and Kang S-W 2016 Structures: liquid crystals *Reference Module in Materials Science and Materials Engineering* Elsevier
[3] Herbert K M, Fowler H E, McCracken J M, Schlafmann K R, Koch J A and White T J 2021 Synthesis and alignment of liquid crystalline elastomers *Nat. Rev. Mater.* **7** 23–38
[4] Yakuphanoglu F, Okutan M, Koysal O, Ahn S M and Keum S R 2008 Dielectric anisotropy, and diffraction efficiency properties of a doped nematic liquid crystal *Dyes & Pig.* **76** 721–5
[5] Singh G, Vijaya Prakash G, Choudhary A and Biradar A M 2010 Homeotropic alignment of nematic liquid crystals with negative dielectric anisotropy *Phys. B Condens. Matter.* **405** 2118–21
[6] Chen H, Liu Y, Chen M, Jiang T, Yang Z and Yang H 2022 Negative dielectric anisotropy liquid crystal with improved photo-stability, anti-flicker, and transmittance for 8K display applications *Mol.* **27** 7150
[7] Adhikari B and Das M K 2013 The role of negative dielectric anisotropy liquid crystalline materials in LCD's *Conference: 5th Asian Conference on Colloid and Interface Science* **1**
[8] Chen Y, Peng F, Yamaguchi T, Song X and Wu S T 2013 High performance negative dielectric anisotropy liquid crystals for display applications *Crystals* **3** 483–503
[9] Sivaranjini B, Mangaiyarkarasi R, Ganesh V and Umadevi S 2018 Vertical alignment of liquid crystals over a functionalized flexible substrate *Scient. Rep.* **8** 1–13
[10] Castellano J A 1983 Surface anchoring of liquid crystal molecules on various substrates *Mol. Cryst. Liq. Cryst.* **94** 33–41
[11] Chaudhari P *et al* 2001 Atomic-beam alignment of inorganic materials for liquid-crystal displays *Nature* **411** 56–9
[12] Wu H Y and Pan R P 2007 Liquid crystal surface alignments by using ion beam sputtered magnetic thin films *Appl. Phys. Lett.* **91** 074102
[13] Lee D W, Lee J H, Kim E M, Heo G S, Kim D H, Oh J Y, Liu Y and Seo D S 2021 Surface modification of a poly(ethylene-co-vinyl acetate) layer by ion beam irradiation for the uniform alignment of liquid crystals *J. Mol. Liq.* **339** 116700
[14] Prakash J, Varshney D, Chauhan S, Kaushik A and Mishra Y K 2023 Progress in radiations induced engineering of liquid crystal properties for high-performance applications, *Phys. Rep.* **105** 1–23
[15] Yaroshchuk O and Reznikov Y 2011 Photoalignment of liquid crystals: basics and current trends *J. Mater. Chem.* **22** 286–300
[16] Takatoh K 2005 *Alignment Technology and Applications of Liquid Crystal Devices* (CRC Press, Taylor and Francis)
[17] Kim D, Ndaya D, Bosire R, Masese F K, Li W, Thompson S M, Kagan C R, Murray C B, Kasi R M and Osuji C O 2022 Dynamic magnetic field alignment and polarized emission of semiconductor nanoplatelets in a liquid crystal polymer *Nat. Comm.* **13** 1–10
[18] Saunders F C, Staromlynska J, Smith G W and Daniel M F 1985 Liquid crystal alignment on langmuir-blodgett films *Mol. Cryst. Liq. Cryst.* **122** 297–308
[19] Priscilla P, Malik P, Supreet A, Kumar R, Castagna G and Singh 2023 Recent advances and future perspectives on nanoparticles-controlled alignment of liquid crystals for displays and other photonic devices *Crit. Revi. Sol. State Mater. Sci.* **48** 57–92
[20] Prakash J, Kumar A and Chauhan S 2022 Aligning liquid crystal materials through nanoparticles: a review of recent progress *Liquids* **2** 50–71
[21] Kinkead B and Hegmann T 2009 Effects of size, capping agent, and concentration of CdSe and CdTe quantum dots doped into a nematic liquid crystal on the optical and electro-optic properties of the final colloidal liquid crystal mixture *J. Mater. Chem.* **20** 448–58
[22] Varshney D, Prakash J and Singh G 2023 Indium tin oxide nanoparticles induced tunable dual alignment in nematic liquid crystal *J. Mol. Liq.* **374** 121264
[23] Qi H, Kinkead B and Hegmann T 2008 Unprecedented dual alignment mode and freedericksz transition in planar nematic liquid crystal cells doped with gold nanoclusters *Adv. Funct. Mater.* **18** 212–21
[24] Varshney D, Prakash J and Singh G 2023 Indium tin oxide nanoparticles induced molecular rearrangement in nematic liquid crystal *J. Mol. Liq.* **387** 122578
[25] Joudeh N and Linke D 2022 Nanoparticle classification, physicochemical properties, characterization, and applications: a comprehensive review for biologists *J. Nanobiotech.* **20** 1–29
[26] Jeng S C, Kuo C W, Wang H L and Liao C C 2007 Nanoparticles-induced vertical alignment in liquid crystal cell *Appl. Phys. Lett.* **91** 061112
[27] Hwang S J, Jeng S C, Yang C Y, Kuo C W and Liao C C 2008 Characteristics of nanoparticle-doped homeotropic liquid crystal devices *J. Phys. D: Appl. Phys.* **42** 025102
[28] Chinky P, Kumar V, Sharma P, Malik K K and Raina 2019 Nano particles induced vertical alignment of liquid crystal for display devices with augmented morphological and electro-optical characteristics *J. Mol. Struct.* **1196** 866–73
[29] Lim Y J, Choi Y E, Kang S W, Kim D Y, Lee S H and Hahn Y B 2013 Vertical alignment of liquid crystals with zinc oxide nanorods *Nanotechnology* **24** 345702
[30] Rai Dogra A, Sharma V and Kumar P 2023 Analysis of morphological and electro-optical properties of silica nanoparticles induced vertically aligned liquid crystal - effect of doping and coating techniques *Mater. Today Proc.* **80** 538–43
[31] Gidwani B, Sahu V, Shukla S S, Pandey R, Joshi V, Jain V K and Vyas A 2021 Quantum dots: prospectives, toxicity, advances and applications *J. Drug Deliv. Sci. Technol.* **61** 102308
[32] Cotta M A 2020 Quantum dots and their applications: what lies ahead? *ACS Appl. Nano Mater.* **3** 64920–4
[33] Singh G, Fisch M and Kumar S 2016 Emissivity and electrooptical properties of semiconducting quantum dots/rods and liquid crystal composites: a review *Rep. Prog. Phys.* **79** 056502
[34] Supreet and Singh G 2020 Recent advances on cadmium free quantum dots-liquid crystal nanocomposites *Appl. Mater Today* **21** 100840
[35] Lee W K, Hwang S J, Cho M J, Park H G, Han J W, Song S, Jang J H and Seo D S 2012 CIS–ZnS quantum dots for self-aligned liquid crystal molecules with superior electro-optic properties *Nanoscale* **5** 193–9
[36] Son I, Son S R, An J, Choi J W, Kim S, Lee W Y and Lee J H 2021 Photoluminescent surface-functionalized graphene quantum dots for spontaneous interfacial homeotropic orientation of liquid crystals *J. Mol. Liq.* **332** 115901
[37] Neha, Singh G, Kumar S, Malik P and Supreet 2023 Recent trends and insights into carbon dots dispersed liquid crystal composites *J. Mol. Liq.* **384** 122225

[38] Urbanski M, Mirzaei J, Sharma A, Hofmann D, Kitzerow H S and Hegmann T 2016 Chemically and thermally stable, emissive carbon dots as viable alternatives to semiconductor quantum dots for emissive nematic liquid crystal–nanoparticle mixtures with lower threshold voltage *Liq. Cryst.* **43** 183–94
[39] Rastogi A, Pandey F P, Hegde G and Manohar R 2020 Time-resolved fluorescence and UV absorbance study on Elaeis guineensis/oil palm leaf-based carbon nanoparticles doped in nematic liquid crystals *J. Mol. Liq.* **304** 112773
[40] Rastogi A, Hegde G, Manohar T and Manohar R 2021 Effect of oil palm leaf-based carbon quantum dot on nematic liquid crystal and its electro-optical effects *Liq. Cryst.* **48** 812–31
[41] Rastogi A, Pandey F P, Parmar A S, Singh S, Hegde G and Manohar R 2021 Effect of carbonaceous oil palm leaf quantum dot dispersion in nematic liquid crystal on zeta potential, optical texture and dielectric properties *J. Nanostruct. Chem.* **11** 527–48
[42] Priscilla P *et al* 2023 Eco-friendly carbon dots induced thermally stable vertical alignment in planar anchored nematic liquid crystal *J. Mol. Liq.* **385** 122318
[43] Priscilla P *et al* 2024 Effect of doping of organo-soluble carbon dots on ionic relaxation and conductivity of planar anchored cyanobiphenyl based nematic liquid crystal *J. Mol. Struct.* **1301** 137403
[44] Zheng B, Liu T, Paau M C, Wang M, Liu Y, Liu L, Wu C, Du J, Xiao D and Choi M M F 2015 One pot selective synthesis of water and organic soluble carbon dots with green fluorescence emission *RSC Adv.* **5** 11667–75
[45] Mahesh P, Shah A, Swamynathan K, Singh D P, Douali R and Kumar S 2020 Carbon dot-dispersed hexabutyloxytriphenylene discotic mesogens: structural, morphological and charge transport behavior *J. Mater. Chem. C Mater.* **8** 9252–61
[46] Minervini G, Panniello A, Fanizza E, Agostiano A, Curri M L and Striccoli M 2020 Oil-dispersible green-emitting carbon dots: new insights on a facile and efficient synthesis *Materials* **13** 3716
[47] Schiekel M F and Fahrenschon K 1971 Deformation of nematic liquid crystals with vertical orientation in electrical fields *Appl. Phys. Lett.* **19** 391–3
[48] Haase W and Wróbel S 2003 *Relaxation Phenomena: Liquid Crystals, Magnetic Systems, Polymers, High-Tc Superconductors, Metallic Glasses* (Springer) 716
[49] Kremer F and Schönhals A 2003 *Broadband Dielectric Spectroscopy* (Springer) 729
[50] Varshney D, Anu, Prakash J, Singh V P, Yadav K and Singh G 2022 Probing the impact of bismuth-titanate based nanocomposite on the dielectric and electro-optical features of a nematic liquid crystal material *J. Mol. Liq.* **347** 118389
[51] Anu D, Varshney K, Yadav J, Prakash H M and Singh G 2022 Tunable dielectric and memory features of ferroelectric layered perovskite Bi4Ti3O12 nanoparticles doped nematic liquid crystal composite *J. Mol. Liq.* **369** 120820
[52] Neha, Singh G, Malik P, Kumar S, Malik P, Singh A K and Supreet 2023 Tunable optical, electro-optical and dielectric properties of eco-friendly graphene quantum dots-nematic liquid crystal composites *Liq. Cryst.* **50** 2345–59
[53] Ansari A A, Prakash J, Nidhi, Aafreen, Chauhan S and Singh G 2024 Effect of perovskite quantum dots on the dielectric properties of a nematic liquid crystal material *Indian J. Pure and Appl. Phys.* **62** 109–15
[54] Parveen A, Prakash J and Singh G 2022 Impact of strontium titanate nanoparticles on the dielectric, electro-optical and electrical response of a nematic liquid crystal *J. Mol. Liq.* **354** 118907
[55] Gulati S, Baul A, Amar A, Wadhwa R, Kumar S and Varma R S 2023 Eco-Friendly and sustainable pathways to photoluminescent carbon quantum dots (CQDs) *Nanomaterials* **13** 554